

## Research Article

# Assessing the Complexity of Potential Bicycle Interference on Vehicles on Urban Road Segments

Shihan Wang , Ying Ni , and Jianqiang Li 

*Department of Traffic Engineering & Key Laboratory of Road and Traffic Engineering, Ministry of Education, Tongji University, Shanghai 201804, China*

Correspondence should be addressed to Ying Ni; [ying\\_ni@tongji.edu.cn](mailto:ying_ni@tongji.edu.cn)

Received 21 March 2023; Revised 2 June 2023; Accepted 24 June 2023; Published 12 July 2023

Academic Editor: Laura Garach

Copyright © 2023 Shihan Wang et al. This is an open access article distributed under the Creative Commons Attribution License, which permits unrestricted use, distribution, and reproduction in any medium, provided the original work is properly cited.

Interacting with bicycles on urban road segments is complex for vehicles, due to the diverse and flexible cycling behavior that can cause interferences. Studies show that driving mixed with bicycles is also a great challenge for autonomous vehicles (AVs), and it is necessary to consider the interference of bicycles when selecting public roads for testing. However, existing road evaluation methods mostly focus on autonomous driving functions and accident analysis, although bicycles have been considered, often with insufficient consideration of their interference. This study analyzes two types of cycling behavior that could interfere with vehicles, including lateral (turning handlebars) and longitudinal (braking or accelerating) behavior, with each occurrence of such behavior considered as one potential lateral or longitudinal interference. From the perspective of cycling behavior, a framework is proposed to assess the complexity of potential bicycle interference on vehicles on road segments. A higher frequency of both potential lateral and longitudinal interference represents a higher complexity of potential interference. A naturalistic field experiment was conducted to collect the potential lateral and longitudinal interference frequency and the environmental parameters of road segments. The quantile regression model was applied to analyze the environmental factors influencing different interference frequencies separately and further establish the assessing model of the potential bicycle interference complexity, and the usability of the model has been demonstrated with a case study. Results show that the potential interference complexity varies across road segments, with some factors leading to more frequent potential lateral and longitudinal interference but with varying degrees of impact (such as the separation between bicycles and vehicles), while some only affect the lateral interference frequency (such as the on-street parking condition). The proposed framework can help autonomous driving companies or evaluation agencies to select appropriate testing roads, thus promoting the development of autonomous driving.

## 1. Introduction

The interaction between vehicles and bicycles on urban road segments can be complex, as bicycles, with their small structure and flexible behavior, tend to cause more uncertain interferences to vehicles [1–4]. With the rapid development of autonomous driving, autonomous vehicles (AVs) are being tested and are even operating commercially on public roadways [5, 6], and the presence of bicycles on mixed traffic roads is likewise a significant challenge. However, the current AVs cannot handle the complex interferences of bicycles perfectly. The National Highway Traffic Safety Administration (NHTSA) reported that there were 130 automated driving systems (ADS) equipped vehicle crashes

during testing on public roads, including 7 crashes with bicycles on urban roadways [7, 8], and the crash rate is relatively high, posing a certain safety threat to road users [9–11]. Therefore, the bicycle interference on vehicles needs to be considered when selecting public roadways for AV driving, and the specific road segment can be further determined according to the functional demands and characteristics of AVs.

Currently, some countries have published public road selection principles for the driving of AVs, mostly based on autonomous driving functions and accident analysis [12, 13], and although bicycles are taken into account, often with insufficient consideration of the interference that bicycles may cause to vehicles. On the other hand, some studies have

considered the behavior of bicycles in roadway complexity assessments [14–18], but they only included factors such as speed, and relative distance, which does not provide an in-depth analysis of the bicycle interference on vehicles. This study considers two types of cycling behavior that could interfere with vehicles, including lateral (turning the handlebars) and longitudinal (braking or accelerating in cycling direction) behavior [19], with each occurrence of such behavior considered as one potential lateral or longitudinal interference. From the perspective of a cycling behavior, a framework for assessing the complexity of potential bicycle interference on vehicles on urban road segments is proposed, and the higher the frequency of the potential lateral and longitudinal interference on the road segment, the higher the potential interference complexity, which can support the selection of public road segments for AV testing and operation. The main contributions of this study can be summarised as follows:

- (1) The environmental factors influencing the frequency of potential lateral and longitudinal bicycle interference on vehicles were analyzed separately, based on the naturalistic field experiment data
- (2) An evaluation model of the complexity of potential bicycle interference on vehicles on road segments was established, by quantifying the lateral and longitudinal interference frequency
- (3) Guidance was provided for selecting the public roadways for AV testing, which can facilitate the improvement of interaction strategies with bicycles

The remainder of this paper is organized as follows: a literature review is presented in Section 2. After reviewing the existing research, the materials and methods are described in Section 3, followed by the results and discussion in Section 4, and finally, conclusions are drawn in Section 5.

## 2. Literature Review

This section presents a review of the studies on the evaluation of road scenarios as well as the analysis of bicycle interference on vehicles.

In the research about autonomous driving road scenarios, scenarios can be understood as the driving environment of intelligent vehicles [20–22], and a lot of work has been performed on the scenario generation [23–27], and the studies on the road segment evaluation are mostly based on accident and autonomous driving function dimensions. On the one hand, some countries have introduced road segment selection principles. For example, the NHTSA provided the precrash scenarios [12]. The European Union combed through the potential and real accident scenarios to summarize the key scenarios for manual and autonomous driving [13]. China published the management specification for intelligent connected vehicle road testing, which specified the items for automatic driving function testing, and further refined the items and scenarios for function testing in response to this specification [13]. Some consortia have graded testing road segments in terms of traffic environment

[13]. However, in these regulations, although bicycles are taken into account, there is no clear definition on the interference complexity of bicycles to vehicles.

On the other hand, scholars have also assessed the road traffic complexity, which is a description and assessment of the surrounding environmental conditions during driver driving and is closely related to the road traffic environment, mainly considering the static and dynamic environmental parameters [17, 28–31], with static including road facilities, weather, and other parameters and dynamic including the behavior of participants. Some studies integrated the static and dynamic parameters. Gao et al. [14–16] first used the information entropy theory to establish a traffic environment complexity model to specifically quantify the static and dynamic complexity of road segments. Zhang et al. [17] calculated the complexity of the environment in special areas using an information entropy-based model. Yang [18] obtained the complexity of the traffic environment based on the grey relation analysis method and improved the gravitation model that introduced the concepts of equivalent mass and the contribution degree of the unmanned vehicles' driving strategy. In the abovementioned studies, bicycles as important road users were considered, but still in a limited way, with factors such as speed and relative distance, there was no in-depth analysis of the cycling behavior that could interfere with vehicles. Compared to the vehicle, which drives along the lane with a relatively simple behavior, bicycles exhibit the following two behavioral characteristics: (1) complex behavioral patterns [2]: when cyclists ride on a road segment, they tend to adopt a variety of behaviors, mainly lateral (turning the handlebars) and longitudinal (braking or accelerating) [32], and these actions tend to have different characteristics and cause different interferences with vehicles [33]. (2) High behavioral uncertainty [3]: bicycles are highly susceptible to the changing behavior, and cyclists may behave differently in different scenarios, which can pose a great challenge for vehicles to cope with them [1, 4], especially AVs. Therefore, the interference caused by bicycles to AVs cannot be ignored when selecting public roadways, which is where this study focuses on.

With regard to the interference of bicycles on vehicles, most existing studies are conducted on the characteristics of mixed traffic flow and traffic impedance, thereby analyzing the impact of bicycles on vehicles from the perspective of traffic flow parameters. Results show that the operational state of bicycle traffic could impact the lateral and longitudinal movements of vehicles, such as causing speed reduction and fluctuation [34–36]. However, few studies analyzed the interference in more detail from the perspective of bicycles. Based on this, the aim of this study is to distinguish the lateral and longitudinal behaviors of bicycles that could interfere with vehicles, to investigate the environmental factors that influence the occurrence of potential bicycle interference, and to further evaluate the complexity of potential bicycle interference on vehicles when the vehicle travels on road segments.

### 3. Materials and Methods

#### 3.1. Data Collection

**3.1.1. Instrumented Probe Bicycle.** An instrumented probe bicycle (IPB) was developed to collect cycling behavior data. To suit different cyclists and capture the vibrations transmitted from road surfaces more realistically, a 24-inch bicycle without shock absorbers was chosen. The bicycle was equipped with an attitude sensor (31.5 mm × 21.5 mm × 9 mm; 10 Hz) and a GPS receiver. The attitude sensor is easy to install and includes a high-precision gyroscope, accelerometer, and geomagnetic field sensor that can measure the acceleration (in the direction of movement), angle (changing the position of the moving object), and angular velocity (rotational speed and direction) in three dimensions [37]. The GPS device is used to collect the speed data. The sensor positions and coordinate system are shown in Figure 1. Rotations (angular motions) of the bicycle around the  $x$ -,  $y$ -, and  $z$ -axis are called pitch, roll, and yaw, respectively.

**3.1.2. Field Experiment.** Data were collected in a naturalistic field experiment in Anting Town, Jiading District, Shanghai, China, comprising 18 segments with environmental differences, as shown in Figure 2(a); to ensure the continuity of cycling, every road segment was considered. The field experiment was conducted for three days in sunny weather from 08:30 to 10:30 and from 15:30 to 17:30. Twenty university students volunteered for the experiment, and their personal socio-demographic information, including their gender and cycling experience level, is shown in Table 1. During the experiments, participants rode the IPB separately on each prescribed route, for a total of six routes ranging from 2.0 to 2.5 km in length (Figure 2(b)). The infrastructure and traffic conditions of these road segments were investigated as the potential factors influencing the occurrence of potential bicycle interference, with references to the existing studies on road scenario evaluation and cycling behavior analysis [13, 38, 39], and the descriptions of the environment information are shown in Table 2. Among them, the traffic volumes were observed in the middle of each road segment, which were further converted to hourly volume, classified as low, medium, and high traffic volumes. The classification criteria for low, medium, and high traffic volumes are referenced from the literature [40].

**3.1.3. Data Preparation.** One complete cycling on a road segment was counted as a trajectory sample. A total of 540 samples were thus obtained, and after screening for the missing data, the final number of valid samples was 342. During the experiment, the acceleration, angle, angular velocity on the three axes, and speed were collected (Table 3), which were used to identify the potential lateral and longitudinal interference frequency for one cycling.

**3.2. Identification of Potential Interference.** In this study, the potential lateral and longitudinal interference was first identified and then the indicators representing the potential

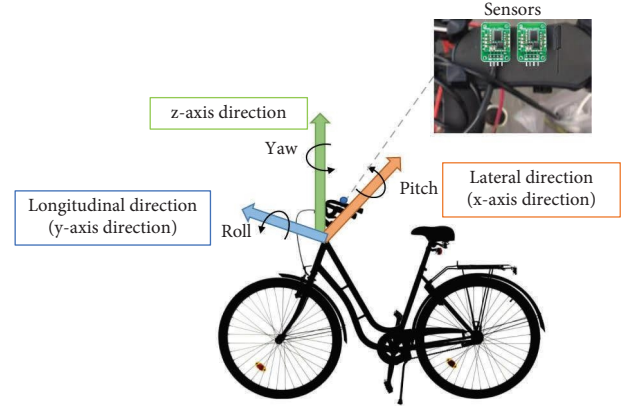


FIGURE 1: IPB-based data collection system.

TABLE 1: Overview of demographic data.

Cycling experience	Gender		Total
	Male	Female	
Highly experienced	4	3	7
Moderately experienced	4	4	8
Inexperienced	2	3	5
Total	10	10	20

interference frequency during cycling were extracted. For road segments with physical separation between vehicles and bicycles, the behavior of the bicycles would not interfere with the vehicles generally, but for road segments without physical separation between vehicles and bicycles, the bicycles tend to influence the vehicles. Therefore, the analysis of potential interference focuses on road segments with no or marking separation from bicycles, and for the former, the whole segment is considered as the interference area of bicycles, while for the latter, only the vehicle lane and the range within one-third of the bicycle lane width from the separation marking are considered as the interference area, as shown in Figure 3.

When the bicycle swings the front with lateral deflection, it tends to put stress on the vehicle, which may interfere with the vehicle's motion. One such lateral behavior in the interference area is considered to have one potential lateral interference. A control experiment was performed on a mixed bicycle-vehicle road, to identify the lateral behavior feature by comparing the variation of the speed and data along the three axes (acceleration, angle, and angular velocity) for stable cycling and obvious lateral deflection cycling. It was found that the change in the  $z$ -axis angle was most significant and could directly reflect the lateral action of bicycles. Based on this, the definition of potential lateral interference is as follows:

$$N_t = \begin{cases} 1, & \frac{(\theta_{zt} - \bar{\theta}_z)}{\sigma} \geq 2 \text{ or } \leq -2, \\ 0, & \text{else.} \end{cases} \quad (1)$$

TABLE 2: Descriptions of the environment of road segments.

Variable	Description	Summary statistics
Separation from vehicles and bicycles	No segregation	8 (44.4%)
	Marking segregation	6 (33.3%)
	Physical segregation	4 (22.2%)
Bicycle lane width	Narrow	4 (22.2%)
	Median	5 (27.8%)
	Wide	9 (50.0%)
Number of entrance and exit points	$\leq 3$	3 (16.7%)
	4–5	6 (33.3%)
	6–10	8 (44.4%)
	$>10$	1 (5.6%)
Land use type	Noncommercial land	11 (61.1%)
	Commercial land	7 (38.9%)
Separation from pedestrians and bicycles	No physical separation	10 (55.6%)
	Physical separation	8 (44.4%)
On-street parking	No parking	95 (27.8%)
	Limited parking (0%–50% of the road area)	142 (41.5%)
	Abundant parking ( $\geq 50\%$ of the road area)	105 (30.7%)
Vehicle volume	Low	116 (33.9%)
	Median	83 (24.3%)
	High	143 (41.8%)
Bicycle volume	Low	111 (32.5%)
	Median	150 (43.9%)
	High	81 (23.7%)
Pedestrian volume	Low	94 (27.5%)
	Median	106 (31.0%)
	High	142 (41.5%)

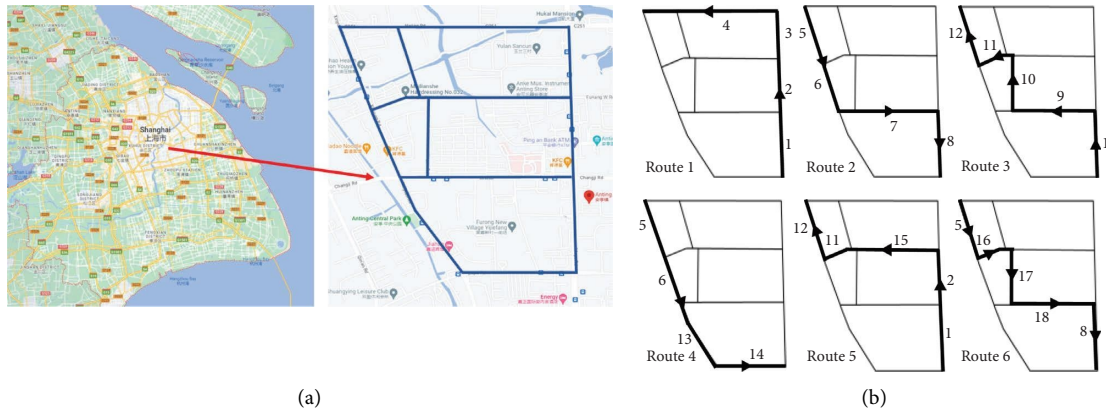


FIGURE 2: Naturalistic field experiment site. (a) Field experiment location. (b) Predefined cycling routes.

where  $N_t$  represents whether the potential lateral interference is present at time  $t$ . Combined with the experimental results and feature meaning [41], it is considered that if the z-score [42] value of the z-axis angle  $\geq 2$  or  $\leq -2$  at time  $t$ , then there is a potential lateral interference with  $N_t = 1$ .

The longitudinal (cycling direction) behavior of bicycles that may cause interference with vehicles is commonly associated with the sudden acceleration and braking, and one such longitudinal behavior in the interference area is considered to have one potential longitudinal interference. Comparing the changes in the speed and three axes' data (acceleration, angle, and

angular velocity) for the accelerating, decelerating, and stable cycling states in the control experiments on the mixed bicycle-vehicle road segment, it was observed that the acceleration along the y-axis could characterize the longitudinal acceleration and braking of bicycles, with significant variations. The y-axis acceleration can reflect the speed fluctuation, compared with the accelerating state, and the variation during deceleration was more dramatic because accelerating requires human pedaling and is opposed by ground friction, whereas decelerating uses brake pads to directly stop the wheel from turning and is assisted by ground friction. Therefore, the maximum deceleration that can be achieved may be greater than the

TABLE 3: Descriptive statistics of relative attitude sensor data.

Attitude sensor data	Average	Min	Max	SD
Pitch ( $^{\circ}$ )	2.92	-7.97	9.25	5.18
Angular velocity along $x$ -axis ( $^{\circ}/s$ )	6.75	0.00	58.78	9.10
Acceleration along $x$ -axis ( $m/s^2$ )	0.64	0.00	5.78	1.24
Roll ( $^{\circ}$ )	0.13	-32.81	30.17	6.70
Angular velocity along $y$ -axis ( $^{\circ}/s$ )	11.51	0.00	83.23	12.07
Acceleration along $y$ -axis ( $m/s^2$ )	2.87	0.00	6.96	2.87
Yaw ( $^{\circ}$ )	3.55	-30.32	33.63	7.10
Angular velocity along $z$ -axis ( $^{\circ}/s$ )	7.35	0.00	76.85	10.79
Acceleration along $z$ -axis ( $m/s^2$ )	3.21	0.00	7.53	2.58
Speed (m/s)	5.45	0.00	8.31	3.26

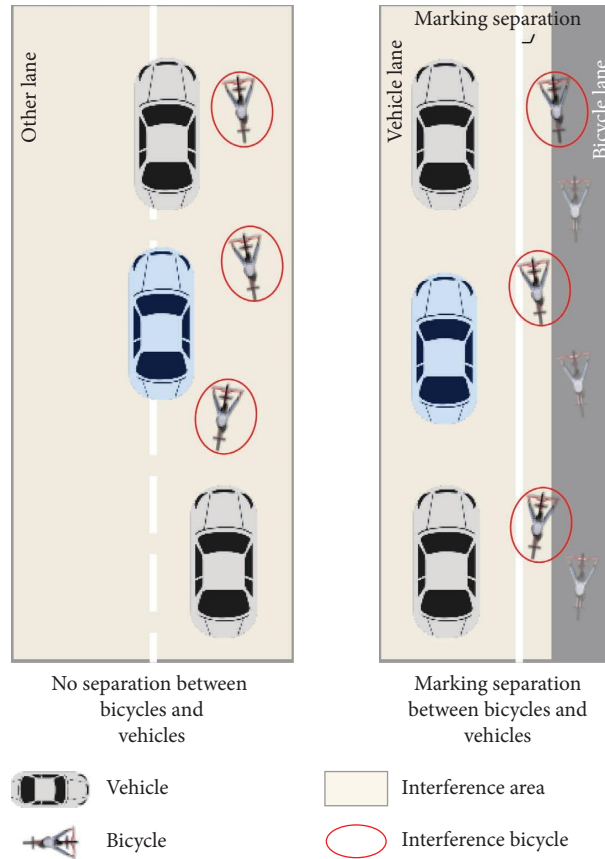


FIGURE 3: Interference area of road segment with no or marking separation between vehicles and bicycles.

maximum acceleration. In addition, this study also explored the relationship between speed magnitude and the potential interference, and the analysis of variance (ANOVA) was conducted to analyze the difference in cycling speed among road segments without physical separation between vehicles and bicycles, and the results revealed a nonsignificant difference in the cycling speed on these road segments with a Sig. value of 0.874, so the speed magnitude was not further considered. Combined with experimental results and the literature [40], the potential longitudinal interference is defined using the  $y$ -axis acceleration as follows:

$$N_{yat+} = \begin{cases} 1, & a_{yt} \geq 0.168g, \\ 0, & \text{else,} \end{cases} \quad (2)$$

$$N_{yat-} = \begin{cases} 1, & a_{yt} \leq -0.294g, \\ 0, & \text{else,} \end{cases}$$

where  $N_{yat+}$  is 1 if there is a potential longitudinal interference related to the acceleration at time  $t$ , or else it is 0; and  $N_{yat-}$  is 1 if there is a potential longitudinal interference related to deceleration at time  $t$ , or else it is 0.

Furthermore, the statistical indicators that could represent the frequency of potential interference during a ride were extracted, including the lateral interference frequency, longitudinal acceleration, and deceleration frequency, as shown in Table 4.

Subsequently, the distribution of  $F_{lat}$ ,  $F_{ya+}$ , and  $F_{ya-}$  on each studied road segment is visualized (Figure 4). Differences were found in the frequency of the potential lateral and longitudinal interference among road segments. On some road segments (e.g., road segment 12), the lateral behavior of bicycles occurred more frequently, whereas on others (e.g., road segment 6), longitudinal deceleration was more frequent. In addition, for most of the investigated road segments, the distribution of  $F_{ya+}$  did not differ significantly, indicating that the deceleration behavior is better than acceleration in distinguishing differences in potential longitudinal interference across road segments. Therefore, the exploration of the potential bicycle interference complexity on vehicles in this study mainly measures  $F_{lat}$  and  $F_{ya-}$ . The distribution of the potential lateral and longitudinal interference (deceleration) frequency is shown in Figure 5, and it has been proven to be convergent, which could understand the overall characteristics of the potential bicycle interference on vehicles on road segments [43].

**3.3. Evaluation Model of Potential Bicycle Interference Complexity.** In order to estimate the complexity of potential bicycle interference on vehicles under different situations, this study applied the quantile regression model for analyzing the frequency of the potential lateral and longitudinal interference separately, with the dependent variable being the potential interference frequency and independent variables being the separation between vehicles and bicycles, separation between pedestrians and bicycles, vehicle volume, bicycle volume, pedestrian volume, bicycle lane width, number of entrance and exit points, land use type, on-street parking condition, and cyclists' experience and gender.

Quantile regression is a method to estimate the relationship between a set of explanatory variables and the quantile of the response variable, which has been widely used in many fields such as economics and medicine recently, and the current applications in the transportation field are focused on accident modelling [44–47] and accident black spot identification [48]. Unlike OLS regression models that describe the influence of explanatory variables on the conditional expectation of the response variable, quantile regression explores the regression influence relationship under different quantile points and examines the influence of explanatory variables on the overall distribution of the response variable, which can tap richer information and can accurately describe the influence of the independent variables on the variation range of the dependent variable and the shape of the conditional distribution. Considering the dispersion of the frequency of potential interference among the road segments, the usage of this quantile regression enables it to cover the predictions for different frequencies.

The quantile function is defined as in equation (3), and the regression model at the  $\tau$ -quantile can be expressed as equations (4) and (5). In this study,  $\tau$  was set as 0.25, 0.5, and

0.75. Considering that the impact of the vehicle volume on cyclists is closely related to the forms of separation from vehicles, as are the pedestrian volume and separation from pedestrians, this study explored their cross-impacting. Then, the prediction range of the potential lateral and longitudinal interference frequency can be obtained by using the model, as equation (6). The potential bicycle interference complexity is further determined with the following rationale. The potential interference frequency is first divided into five discrete levels (I–V) by considering the lateral and longitudinal interference comprehensively, where the classification of each level is divided by 10 and 20 (the larger frequency demonstrated in the experimental data). Taking into account that the lateral behavior of bicycles makes vehicles more difficult to handle and predict [3, 49], so the area with more potential lateral interferences is designated as level III; in addition, once one interference frequency exceeds 20, it is uniformly set as level V. The final complexity value can be determined as a continuous value based on the proportion of the rectangle composed of the two frequency ranges for each level with equation (7), and the schematic diagram is shown in Figure 6, where the four red curves represent the upper and lower limits of the potential lateral and longitudinal interference frequency and the blue area is the composed rectangle.

$$Q(\tau) = \inf\{y: F(y) \geq \tau\}, \tau \in (0, 1), \quad (3)$$

where the distribution function  $F(y) = P(Y \leq y)$  pertains to the response variable  $Y$ , with  $\tau \in (0, 1)$ .  $Q(\tau)$  is the  $\tau$ -quantile of  $Y$ ; for example,  $\tau = 0.5$  represents the second quartile.

$$Q(\tau | x) = x^T \beta_\tau, \quad (4)$$

where

$$\begin{aligned} \hat{\beta}_\tau = \operatorname{argmin} & \sum_{y_i \geq x_i^T \beta_\tau} \tau(y_i - x_i^T \beta_\tau) \\ & + \sum_{y_i < x_i^T \beta_\tau} (\tau - 1)(y_i - x_i^T \beta_\tau), \end{aligned} \quad (5)$$

where  $x$  is a  $p$ -dimensional vector,  $Q(\tau | x)$  denotes the quantile of the response variable at the  $\tau$ -probability level given the explanatory variable  $x$ ,  $\beta_\tau$  is a vector of the coefficients at the  $\tau$ -quantile, and  $\hat{\beta}_\tau$  is the regression coefficient estimator.

$$F_k = \begin{cases} \left[ \sum_{Latp=1}^{LatP} \frac{Q_{Latp}(0.25 | x)}{N(LatP)}, \sum_{Latp=1}^{LatP} \frac{Q_{Latp}(0.75 | x)}{N(LatP)} \right], \\ \left[ \sum_{Lonp=1}^{LonP} \frac{Q_{Lonp}(0.25 | x)}{N(LonP)}, \sum_{Lonp=1}^{LonP} \frac{Q_{Lonp}(0.75 | x)}{N(LonP)} \right], \end{cases} \quad (6)$$

where  $F_k$  is the potential interference frequency range of the  $k$ th road segment,  $Latp$  is the category of personal attributes that are significantly correlated with the potential lateral interference, and  $N(LatP)$  is the total number of categories of personal attributes to be considered.  $Lonp$  and  $N(LonP)$  are the parameters of potential longitudinal interference.

TABLE 4: Frequency of potential interference for one cycling.

Feature	Description	Average	Min	Max	SD
<i>Potential lateral interference</i>					
$F_{lat}$	Frequency of potential lateral interference for one cycling, lateral times per km	10.96	0.00	26.67	7.51
<i>Potential longitudinal interference</i>					
$F_{ya+}$	Frequency of potential longitudinal interference about accelerating for one cycling, acceleration times per km	2.85	0.00	13.67	2.60
$F_{ya-}$	Frequency of potential longitudinal interference about decelerating for one cycling, deceleration times per km	12.69	1.87	27.00	4.98

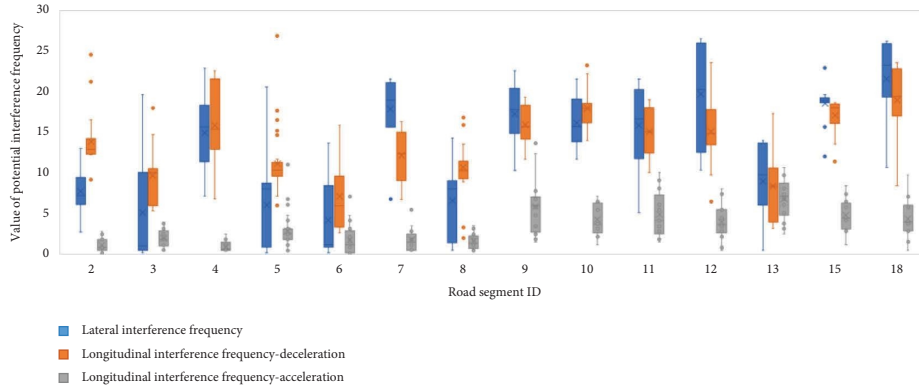
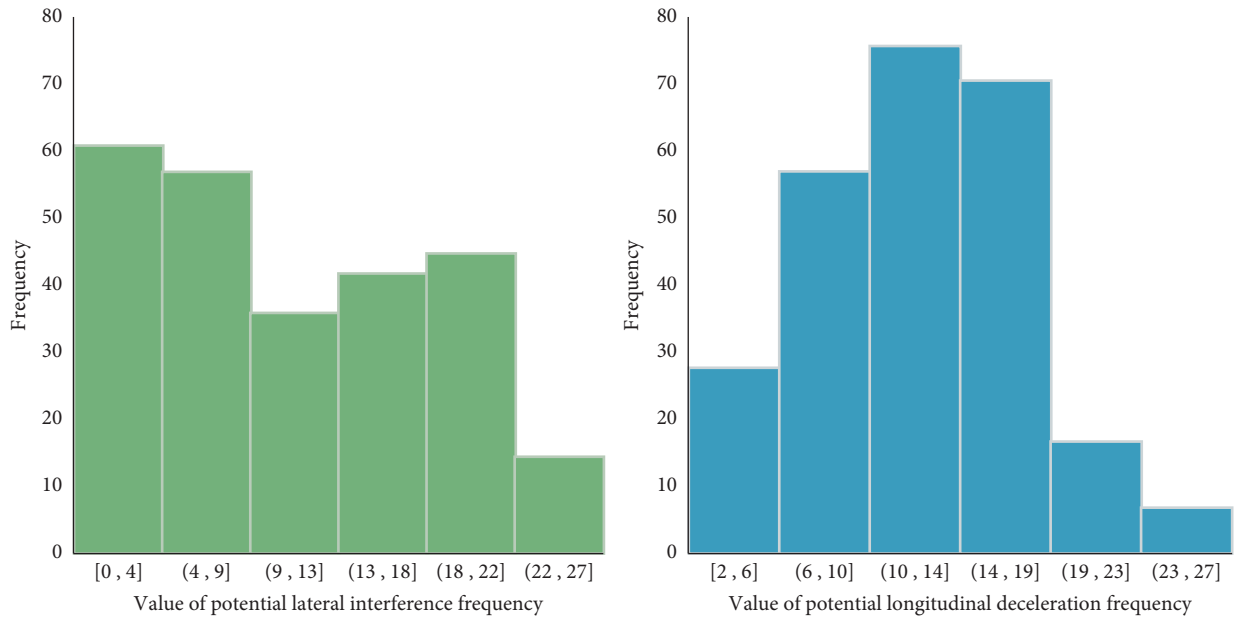
FIGURE 4: Box plots of  $F_{lat}$ ,  $F_{ya+}$ , and  $F_{ya-}$  for each road segment.

FIGURE 5: The distribution of the potential lateral and longitudinal interference frequency.

$$C_k = \left( \sum_i \frac{(S_i \cdot i)}{S} \right) * B_V, \quad (7)$$

where  $C_k$  is the potential bicycle interference complexity and  $i$  is the level occupied by the rectangle consisting of the upper and lower limits of the potential lateral and longitudinal

interference frequency for the  $k$ th road segment, taking values in the range of 1–5.  $S_i$  is the area of the rectangle belonging to the level  $i$ , and  $S$  is the area of the rectangle.  $B_V$  is the bicycle volume level, which is categorized as low, medium, and high, with corresponding values of 1, 2, and 3, respectively.

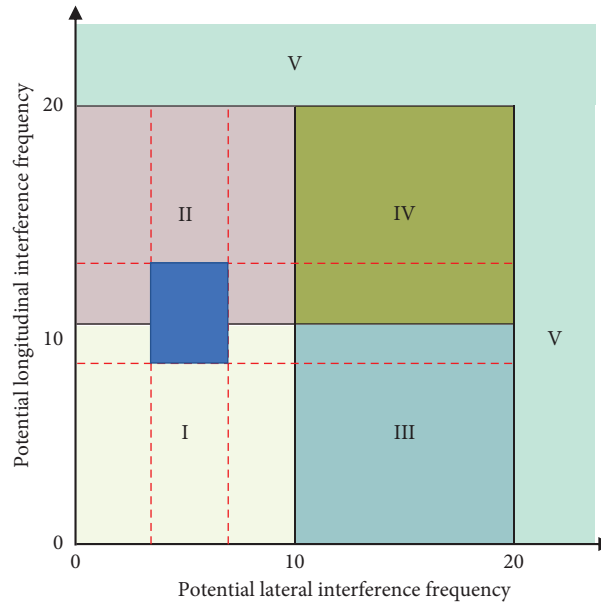


FIGURE 6: Schematic diagram of potential bicycle interference complexity.

## 4. Results and Discussion

**4.1. Results of the Quantile Regression Model.** The estimated coefficients and significance of the model for the potential lateral and longitudinal interference frequency are shown in Tables 5 and 6, respectively, where a positive coefficient for an independent variable indicates that the presence of this variable leads to an increased probability of a higher frequency compared to the base variable, while a negative coefficient indicates a decreased probability.

For the potential lateral interference frequency, eight variables have significant effects, but the significance and coefficients vary by quartile. Bicycle volume, on-street parking condition, number of entrances and exits, land use type, and cycling experience have significant effects on the frequency at each quartile, while bicycle lane width, separation between vehicles and bicycles-vehicle volume, and separation between pedestrians and bicycles-pedestrian volume are only significant at some quartile points. For the longitudinal interference frequency, there are also eight variables that are significantly correlated, but the significant relationships as well as the coefficients are different from the lateral model, where bicycle lane width, number of entrances and exits, land use type, and gender are correlated for all quartiles, and bicycle volume, separation between vehicles and bicycles-vehicle volume, separation between pedestrians and bicycles-pedestrian volume, and cycling experience are significant in some quartiles. The effects of the above-mentioned factors on the potential interference frequency at different quartiles are different. A comparison of the quantile regression coefficients of some significantly correlated variables for the two models is shown in Figure 7. The details of the analysis are as follows.

The growth of the bicycle volume and on-street parking would increase the frequency of potential lateral interference, probably because these factors lead to an increase

in surrounding disturbances that can affect the cycling behavior, which is consistent with the literature [38, 39, 50]. Besides, it has also been found that the coefficient tends to increase with the increase of the quantile, indicating that the cyclists with many lateral actions may be more sensitive to the surrounding traffic, with a more volatile behavior when encountering more bicycles or parking vehicles during cycling. For the frequency of potential longitudinal interference, the effect of a high bicycle volume is close to that of the lateral interference, but the median bicycle volume and on-street parking are not significant. In addition, the wider bicycle lane width would also cause the increase in the frequency of the potential lateral interference, but for the longitudinal, the reduction in the bicycle lane width would increase the frequency. This may be because the narrow road limits the lateral movement and cyclists rely more on deceleration to change their behavior. The findings further enrich the existing knowledge that reducing the effective cycling width would affect the cycling behavior [38, 50, 51].

The more the number of entrances and exits on a road segment, the more likely the cyclists are to encounter the sudden appearance of obstructions, which may lead to more frequent lateral movement or sharp braking [13, 39, 51], and thus more potential lateral and longitudinal interference to vehicles. Besides this, this study also finds that the value of the coefficient for the number of entrances and exits reduces as the quantile increases, implying that they have a greater impact on the low-frequency interference. For the land use type, the lateral and longitudinal interference frequency of bicycles would also significantly increase when the cycling segment is surrounded by the commercial land, probably due to the higher traffic volume around it, which affects the behavior of bicycles, as mentioned in the literature [38, 39], and thus interferes with vehicles. However, the coefficient tends to increase with the increase of the quantile, which has more influence on the high frequency.



TABLE 5: Model result of the potential lateral interference frequency.

Variable (base)	Quantile (sig.)		
	0.25	0.50	0.75
<i>Const</i>	-2.122 (0.083*)	3.111 (0.003***)	8.178 (0.000***)
<i>Separation from vehicle-vehicle volume (marking separation-low volume)</i>			
Marking separation-high vehicle volume-VMh	6.626 (0.000***)	3.379 (0.000***)	1.460 (0.035**)
Marking separation-median vehicle volume-VMm	3.654 (0.000***)	1.576 (0.008***)	0.374 (0.586)
No separation-high vehicle volume-VNh	6.792 (0.000***)	4.455 (0.000***)	6.277 (0.000***)
No separation-median vehicle volume-VNm	5.963 (0.000***)	3.286 (0.000***)	-0.448 (0.579)
No separation-low vehicle volume-VNl	3.999 (0.000***)	0.599 (0.401)	-3.122 (0.000***)
<i>Bicycle lane width (wide)</i>			
Median-BLm	-0.707 (0.180)	-1.112 (0.020**)	-1.228 (0.047**)
Narrow-BLn	-3.091 (0.000***)	-3.118 (0.000***)	-1.993 (0.002***)
<i>Bicycle volume (low)</i>			
High-BVh	1.297 (0.020**)	4.907 (0.000***)	6.892 (0.000***)
Median-BVm	3.480 (0.000***)	3.935 (0.000***)	4.352 (0.000***)
<i>On-street parking (no)</i>			
Abundant-OPa	0.964 (0.038**)	1.364 (0.000***)	1.355 (0.004***)
Limited-OPl	3.147 (0.000***)	3.677 (0.000***)	3.790 (0.000***)
<i>Cycling experience (inexperienced)</i>			
Highly experienced-He	-2.553 (0.000***)	-2.815 (0.000***)	-2.900 (0.000***)
Moderately experienced-Me	-1.257 (0.024**)	-1.378 (0.001***)	-1.082 (0.019**)
<i>Gender (female)</i>			
Male-Gm	0.296 (0.407)	0.292 (0.364)	-0.167 (0.671)
<i>Number of entrance and exit points-Ee</i>	0.543 (0.000***)	0.435 (0.000***)	0.120 (0.068*)
<i>Land use type(noncommercial)</i>			
Commercial-Lc	1.810 (0.000***)	2.160 (0.000***)	2.687 (0.000***)
<i>Separation from pedestrian-pedestrian volume (physical separation-low pedestrian volume)</i>			
Physical separation-high pedestrian volume-PPh	2.260 (0.000***)	1.148 (0.008***)	0.333 (0.526)
Physical separation-median pedestrian volume-PPm	2.260 (0.013**)	-0.103 (0.886)	0.144 (0.875)
No physical separation-high pedestrian volume-PNh	4.499 (0.000***)	3.045 (0.000***)	2.362 (0.004***)
No physical separation-median pedestrian volume-PNm	4.982 (0.000***)	3.069 (0.000***)	2.064 (0.006***)
No physical separation-low pedestrian volume-PNl	3.805 (0.000***)	2.264 (0.000***)	0.503 (0.476)

\*\*\*Significant at the 99% level; \*\*Significant at the 95% level; \*Significant at the 90% level.

TABLE 6: Model result of the potential longitudinal interference frequency.

Variable (base)	Quantile (sig.)		
	0.25	0.50	0.75
<i>Const</i>	3.329 (0.036**)	0.356 (0.823)	5.907 (0.000***)
<i>Separation from vehicle-vehicle volume (marking separation-low volume)</i>			
Marking separation-high vehicle volume-VMh	2.861 (0.004***)	4.616 (0.000***)	4.174 (0.000***)
Marking separation-median vehicle volume-VMm	2.775 (0.002***)	2.827 (0.002***)	1.846 (0.029**)
No separation-high vehicle volume-VNh	2.214 (0.044**)	6.698 (0.000***)	6.166 (0.000***)
No separation-median vehicle volume-VNm	-0.543 (0.597)	5.219 (0.000***)	4.384 (0.000***)
No separation-low vehicle volume-VNl	0.564 (0.609)	4.216 (0.000***)	2.974 (0.004***)
<i>Bicycle lane width (wide)</i>			
Median-BLm	1.112 (0.078*)	2.669 (0.000***)	3.771 (0.000***)
Narrow-BLn	3.674 (0.000***)	5.004 (0.000***)	2.812 (0.000***)
<i>Bicycle volume (low)</i>			
High-BVh	1.703 (0.009***)	2.230 (0.002***)	2.051 (0.004***)
Median-BVm	0.000 (1.000)	0.494 (0.396)	-0.082 (0.881)
<i>On-street parking (no)</i>			
Abundant-OPa	-0.275 (0.687)	-0.170 (0.824)	0.770 (0.314)
Limited-OPl	-0.315 (0.602)	0.234 (0.693)	0.416 (0.490)
<i>Cycling experience (inexperienced)</i>			
Highly experienced-He	-0.777 (0.196)	-1.014 (0.097*)	-1.470 (0.007***)
Moderately experienced-Me	-0.225 (0.719)	-0.344 (0.587)	-1.812 (0.001***)

TABLE 6: Continued.

Variable (base)	Quantile (sig.)		
	0.25	0.50	0.75
<i>Gender (female)</i>			
Male-Gm	-2.157 (0.000***)	-2.532 (0.000***)	-1.457 (0.002***)
<i>Number of entrance and exit points-Ee</i>			
	0.373 (0.000***)	0.300 (0.000***)	0.272 (0.001***)
<i>Land use type (noncommercial)</i>			
Commercial-Lc	2.861 (0.000***)	4.122 (0.000***)	2.137 (0.000***)
<i>Separation from pedestrian-pedestrian volume (physical separation-low pedestrian volume)</i>			
Physical separation-high pedestrian volume-PPh	2.384 (0.000***)	0.905 (0.171)	-0.309 (0.633)
Physical separation-median pedestrian volume-PPm	1.504 (0.129)	-0.762 (0.488)	3.424 (0.001***)
No physical separation-high pedestrian volume-PNh	4.179 (0.000***)	6.920 (0.000***)	5.819 (0.000***)
No physical separation-median pedestrian volume-PNm	4.740 (0.000***)	6.410 (0.000***)	4.190 (0.000***)
No physical separation-low pedestrian volume-PNl	0.568 (0.533)	3.971 (0.000***)	1.568 (0.063*)

\*\*\*Significant at the 99% level, \*\*Significant at the 95% level, and \*Significant at the 90% level.

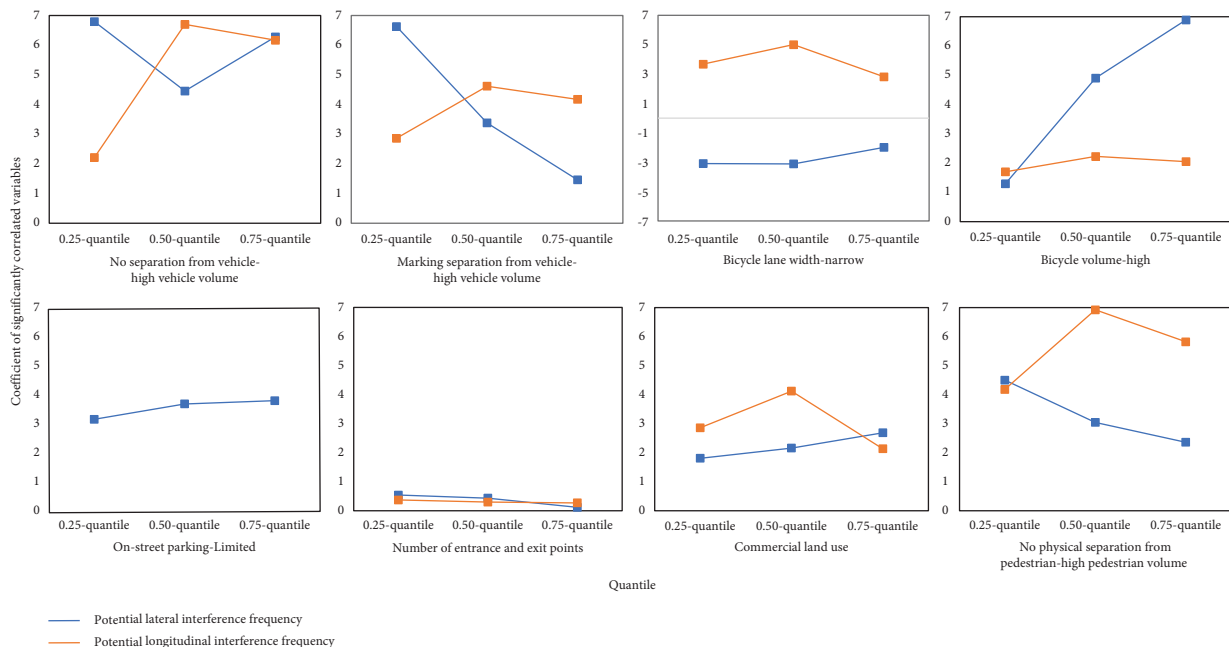





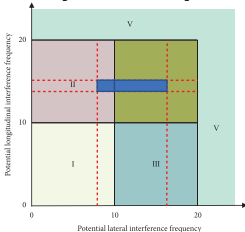
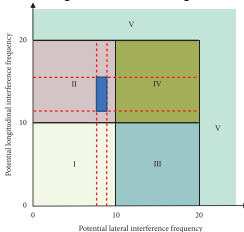
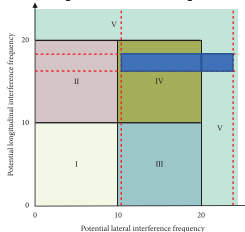
FIGURE 7: A comparison of the coefficients of some significantly correlated variables for the two models.

For the crossover variable of separation between vehicles and bicycles-vehicle volume, the effect on the frequency of potential lateral and longitudinal interference varies by situation. When there is a marking separation, compared to the low vehicle volume, the higher vehicle volume would increase the frequency of lateral and longitudinal interference, especially the low-quantile frequency of lateral and median-quantile frequency of longitudinal. When there is no separation, compared to the marking separated with a low vehicle volume environment, the high vehicle volume significantly increases the lateral and longitudinal interference to vehicles; the moderate volume also tends to cause an increase in interference, mainly for the low-frequency lateral and high-frequency longitudinal interference; and a low vehicle volume would reduce the high frequency, increase the low-frequency lateral interference,

and increase the high-frequency longitudinal interference. It can be seen that in the absence of a physical segregation, vehicle traffic has a significant impact on the cycling behavior, and the cycling behavior can in turn interfere with the vehicle operation. When vehicles operate on road segments that are physically separated from bicycles, there is least interaction between them, and the findings are consistent with the existing research on rating road segments for autonomous driving [13] and exploring factors influencing cycling behavior [51–54].

The effect of different combinations of pedestrian-bicycle separated forms and pedestrian volume on the potential lateral and longitudinal interference frequency also varies. When there is a physical separation, compared to the low pedestrian volume, the moderate volume has a positive effect on the low-quantile lateral and high-quantile longitudinal interference

TABLE 7: Case description.

Variable	Road segment 1	Road segment 2	Road segment 3
Street view			
Separation from vehicles and bicycles	Marking	No separation	No separation
Vehicle volume	Median	Low	High
Bicycle lane width	Median	Narrow	Narrow
Bicycle volume	High	Median	High
On-street parking	Limited	No	Abundant
Number of entrance and exit points	2	2	3
Land use type	Commercial	Noncommercial	Commercial
Separation from pedestrians and bicycles	Physical	No	Physical
Pedestrian volume	High	Median	High
Potential interference frequency-lateral	[7.68, 16.80]	[7.06, 8.39]	[10.45, 24.74]
Potential interference frequency-longitudinal	[13.83, 14.98]	[11.41, 15.15]	[15.83, 18.34]
Schematic			
Complexity of potential interference	10.47	4.00	12.99

frequency, and when the volume is high, there is an increase in both the lateral and longitudinal frequency at a low quantile, perhaps due to the presence of more pedestrians that cause bicycles to fluctuate psychologically, even though there is a separation between them. For the cases of no separation between pedestrians and bicycles, compared to the physical separation with a low pedestrian volume environment, the low-frequency lateral and high-frequency longitudinal interference increases at a low pedestrian volume, while when the pedestrian volume further increases, the lateral and longitudinal interference frequency at both the low-quantile and high-quantile levels would increase. These findings further enrich the existing studies about rating road segments for autonomous driving [13] and analyzing pedestrians' effects on cycling behavior [51, 54, 55].

The model also takes into account the cycling experience and gender of cyclists, and the results show that more experienced cyclists are able to reduce the frequency of potential lateral and longitudinal interference, which is consistent with the previous research that experienced cyclists are more adaptive to road conditions and can ride more smoothly [19]. In addition, female cyclists are found to perform deceleration more frequently than male cyclists, which is consistent with their reported less aggressive behavior [56].

In summary, compared to existing studies, this study analyzes the impact of the road environment on the potential bicycle interference frequency on vehicles comprehensively and explores the lateral and longitudinal interference

separately. Different road environments lead to different potential interferences, and the same environment also has different effects on the interference frequency in different quantiles. For road segments without physical separation between vehicles and bicycles, the presence of high-frequency lateral and longitudinal interferences can cause adverse effects on vehicle operation, and it is important for AVs to carefully select the road segments for testing.

4.2. Evaluation Results of Potential Bicycle Interference Complexity. Based on the model results, this study further gives the complexity calculation method for the potential bicycle interference on vehicles on road segments. The evaluation is implemented in the following steps: (1) Step 1: we obtain the cycling environment of a road segment at a certain time. (2) Step 2: we input the environmental parameters and calculate the predicted potential interference frequency for each quantile under specific conditions. (3) Step 3: we calculate the complexity of the road segment. The model application method is further illustrated by an example that follows, with the sample data from three road segments outside the modelled data, and the results are shown in Table 7.

From the results, it can be seen that the upper limit of the potential lateral interference frequency for road segment 2 is the smallest of the three segments, but the upper limit for the longitudinal lateral interference frequency is not the smallest; thus, the lateral and longitudinal interference of one road

segment may not be consistent, indicating that the potential interference complexity cannot be comprehensively evaluated by a single indicator alone. Based on the calculation method, the complexity for road segment 1 is 10.47, for road segment 2 is 4.00, and for road segment 3 is 12.99. The results are in line with the knowledge and demonstrate that the evaluation framework proposed in this study can achieve the differentiation of potential bicycle interference complexity on vehicles on road segments, which is beneficial for the selection of roads for public testing of AVs.

## 5. Conclusions

As AVs enter open roadways, the interaction with bicycles for vulnerable road users must be taken into account. This study evaluates the complexity of potential bicycle interference on vehicles on road segments from the perspective of a cycling behavior, which can guide the public open road selection of AVs. A naturalistic field experiment based on a compact IPB was conducted to identify the potential lateral and longitudinal interference occurring on the road segment and to further explore the traffic environment factors influencing different interference frequencies, respectively, by using the quantile regression model. The analysis shows that the frequency of the potential lateral and longitudinal interference is different on various road segments, and the separation form between vehicles and bicycles-vehicle volume, separation form between pedestrians and bicycles-pedestrian volume, bicycle lane width, bicycle volume, number of entrances and exits, land use type, and cycling experience all affect the lateral and longitudinal interference frequency, but there are variations in the influence extent, while only on-street parking has the effect on the lateral interference. Based on the model results, a method for evaluating the potential interference complexity is further given, which can determine the complexity based on the traffic environment of the road segment to be evaluated, providing valuable guidance for selecting appropriate roads for public testing of autonomous driving, thereby promoting the development of AVs effectively.

In addition, the evaluation framework can also be extended to other regions, and the IPB developed in this study offers reproducibility by enabling the installation of attitude sensors on other bicycles or even shared bicycles to extract more cycling data for evaluating the potential interference complexity of other regions. However, the quantification of potential interference frequency and the traffic environment parameters to be considered need to be fine-tuned to the local road environment. In the future, efforts will be made to refine the evaluation model to consider the bicycle type and vehicle speed and to further extend it to intersections, thereby forming a comprehensive evaluation of the complexity of potential bicycle interference on vehicles on road networks.

## Data Availability

The experimental data used to support the findings of this study are available from the corresponding author upon request.

## Conflicts of Interest

The authors declare that they have no conflicts of interest.

## Authors' Contributions

Shihan Wang and Ying Ni conceptualized and designed the study, drafted and prepared the manuscript, and analysed and interpreted the results. Shihan Wang and Jianqiang Li collected the data. Shihan Wang, Ying Ni, and Jianqiang Li performed the model estimation. All authors reviewed the results and approved the final version of the manuscript.

## Acknowledgments

This research was sponsored by the National Natural Science Foundation of China (Grant nos. 52272313 and 52072262).

## References

- [1] L. Bai, P. Liu, Y. Chen, X. Zhang, and W. Wang, "Comparative analysis of the safety effects of electric bikes at signalized intersections," *Transportation Research Part D: Transport and Environment*, vol. 20, pp. 48–54, 2013.
- [2] X. Yang, B. Wang, and Z. Qin, "Floor field model based on cellular automata for simulating indoor pedestrian evacuation," *Mathematical Problems in Engineering*, vol. 2015, Article ID 820306, 10 pages, 2015.
- [3] W. Zhan, A. D. L. Fortelle, Y. T. Chen, C. Y. Chan, and M. Tomizuka, "Probabilistic prediction from planning perspective: problem formulation, representation simplification and evaluation metric," in *Proceedings of the 2018 IEEE Intelligent Vehicles Symposium (IV)*, pp. 1150–1156, Changshu, China, June 2018.
- [4] Y. Li, L. Xing, W. Wang, M. Liang, and H. Wang, "Evaluating the impact of Mobike on automobile-involved bicycle crashes at the road network level," *Accident Analysis & Prevention*, vol. 112, pp. 69–76, 2018.
- [5] J. Wang, L. Zhang, Y. Huang, J. Zhao, and F. Bella, "Safety of autonomous vehicles," *Journal of Advanced Transportation*, vol. 2020, Article ID 8867757, 13 pages, 2020.
- [6] D. J. Fagnant and K. Kockelman, "Preparing a nation for autonomous vehicles: opportunities, barriers and policy recommendations," *Transportation Research Part A: Policy and Practice*, vol. 77, pp. 167–181, 2015.
- [7] National Highway Traffic Safety Administration (Nhtsa), "Summary report: standing general order on crash reporting for level 2 advanced driver assistance systems," 2022, <https://www.nhtsa.gov/sites/nhtsa.gov/files/2022-06/ADAS-L2-SGO-Report-June-2022.pdf>.
- [8] National Highway Traffic Safety Administration (Nhtsa), "Summary report: standing general order on crash reporting for automated driving systems," 2022, <https://www.nhtsa.gov/sites/nhtsa.gov/files/2022-06/ADS-SGO-Report-June-2022.pdf>.
- [9] T. Götschi, A. Castro, M. Deforth, L. Miranda-Moreno, and S. Zangenehpour, "Towards a comprehensive safety evaluation of cycling infrastructure including objective and subjective measures," *Journal of Transport & Health*, vol. 8, pp. 44–54, 2018.
- [10] A. M. Hezaveh, M. F. Zavareh, C. R. Cherry, and T. Nordfjærn, "Errors and violations in relation to bicyclists' crash risks: development of the bicycle rider behavior

- questionnaire (BRBQ),” *Journal of Transport & Health*, vol. 8, pp. 289–298, 2018.
- [11] World Health Organization, “Global status report on road safety 2018,” 2018, <https://www.who.int/publications/i/item/9789241565684>.
- [12] W. G. Najm and D. L. Smith, “Definition of a pre-crash scenario typology for vehicle safety research,” in *Proceedings of the 20th International Technical Conference on the Enhanced Safety of Vehicles (ESV)*, Lyon, France, August 2007.
- [13] R. Wang, Y. Sun, and J. Song, “Evaluation method and test verification of road test scenes for Autonomous Vehicles (in Chinese),” *Automotive Engineering*, vol. 43, no. 4, pp. 620–628, 2021.
- [14] X. Gao, G. Dong, and L. Gao, “Comparison on driving behavior between manned and unmanned ground vehicles,” in *Proceedings of the 2011 2nd International Conference on Intelligent Control and Information Processing*, pp. 522–526, Harbin, China, June 2011.
- [15] X. Gao, G. Dong, and L. Gao, “Fuzzy synthetic evaluation of driving abilities for intelligent vehicles,” in *Proceedings of the 2011 IEEE 2nd International Conference on Software Engineering and Service Science*, pp. 449–452, Beijing, China, December 2011.
- [16] X. Gao, L. Gao, and G. Dong, “Research on intelligent driving behavior based on cognitive science and scene simulation,” in *Proceedings of the 2011 International Conference on Intelligence Science and Information Engineering*, pp. 226–229, Wuhan, China, July 2011.
- [17] X. Zhang, Y. Zhao, L. Gao, and D. Hao, “Evaluation framework and method of the intelligent behaviors of unmanned ground vehicles based on AHP scheme,” *Applied Mechanics and Materials*, vol. 721, pp. 476–480, 2014.
- [18] S. Yang, L. Gao, Y. Zhao, and X. Li, “Research on the quantitative evaluation of the traffic environment complexity for unmanned vehicles in urban roads,” *IEEE Access*, vol. 9, pp. 23139–23152, 2021.
- [19] A. Feizi, J. Oh, V. Kwizile, and S. Joo, “Cycling environment analysis by bicyclists’ skill levels using instrumented probe bicycle (IPB),” *International Journal of Sustainable Transportation*, vol. 14, no. 9, pp. 722–732, 2020.
- [20] R. H. Moss, J. A. Edmonds, K. A. Hibbard et al., “The next generation of scenarios for climate change research and assessment,” *Nature*, vol. 463, no. 7282, pp. 747–756, 2010.
- [21] S. Geyer, M. Baltzer, B. Franz et al., “Concept and development of a unified ontology for generating test and use-case catalogues for assisted and automated vehicle guidance,” *IET Intelligent Transport Systems*, vol. 8, no. 3, pp. 183–189, 2014.
- [22] T. Menzel, G. Bagschik, and M. Maurer, “Scenarios for development, test and validation of Automated Vehicles,” in *Proceedings of the 2018 IEEE Intelligent Vehicles Symposium (IV)*, pp. 1821–1827, Changshu, China, June 2018.
- [23] H. Shu, K. Yuan, H. Xiu, Q. Xia, and S. He, “Construction of basic test scenarios of Automated Vehicles,” *China Journal of Highway and Transport*, vol. 32, no. 11, pp. 245–254, 2019.
- [24] S. Feng, Y. Feng, C. Yu, Y. Zhang, and H. X. Liu, “Testing scenario library generation for connected and Automated Vehicles, Part I: methodology,” *IEEE Transactions on Intelligent Transportation Systems*, vol. 22, no. 3, pp. 1573–1582, 2021.
- [25] W. Ding, M. Xu, and D. Zhao, “CMTS: a conditional multiple trajectory synthesizer for generating safety-critical driving scenarios,” in *Proceedings of the 2020 IEEE International Conference on Robotics and Automation (ICRA)*, pp. 4314–4321, Paris, France, January 2020.
- [26] A. Calò, P. Arcaini, S. Ali, F. Hauer, and F. Ishikawa, “Generating avoidable collision scenarios for testing Autonomous Driving Systems,” in *Proceedings of the 2020 IEEE 13th International Conference on Software Testing, Validation and Verification (ICST)*, pp. 375–386, Porto, Portugal, September 2020.
- [27] J. Duan, F. Gao, and Y. He, “Test scenario generation and optimization technology for intelligent driving systems,” *IEEE Intelligent Transportation Systems Magazine*, vol. 14, no. 1, pp. 115–127, 2022.
- [28] I. Tang and T. P. Breckon, “Automatic road environment classification,” *IEEE Transactions on Intelligent Transportation Systems*, vol. 12, no. 2, pp. 476–484, 2011.
- [29] Y. Sun, G. Tao, G. Xiong, and H. Chen, “The Fuzzy-AHP evaluation method for unmanned ground vehicles,” *Applied Mathematics & Information Sciences*, vol. 7, no. 2, pp. 653–658, 2013.
- [30] M. Naumann, M. Lauer, and C. Stiller, “Generating comfortable, safe and comprehensible trajectories for Automated Vehicles in mixed traffic,” in *Proceedings of the 2018 21st International Conference on Intelligent Transportation Systems (ITSC)*, pp. 575–582, Maui, HI, USA, May 2018.
- [31] M. Tlig, M. Machin, R. Kerneis et al., “Autonomous Driving System: model based safety analysis,” in *Proceedings of the 2018 48th Annual IEEE/IFIP International Conference on Dependable Systems and Networks Workshops (DSN-W)*, pp. 2–5, Luxembourg, Europe, June 2018.
- [32] R. Utriainen, S. O’Hern, and M. Pöllänen, “Review on single-bicycle crashes in the recent scientific literature,” *Transport Reviews*, vol. 43, no. 2, pp. 159–177, 2023.
- [33] Y. Ni, L. Xin, and K. Long, “Modeling and simulation of right-turning vehicle-bicycle interactions at intersections (in Chinese),” *Journal of Tongji University*, vol. 47, no. 7, pp. 994–1003, 2019.
- [34] J. R. Klop and A. J. Khattak, “Factors influencing bicycle crash severity on two-lane, undivided roadways in North Carolina,” *Transportation Research Record*, vol. 1674, no. 1, pp. 78–85, 1999.
- [35] Y. Luo, B. Jia, J. Liu, W. H. K. Lam, X. Li, and Z. Gao, “Modeling the interactions between car and bicycle in heterogeneous traffic,” *Journal of Advanced Transportation*, vol. 49, no. 1, pp. 29–47, 2015.
- [36] Z. Pu, Z. Li, Y. Wang, M. Ye, and W. Fan, “Evaluating the interference of bicycle traffic on vehicle operation on urban streets with bike lanes,” *Journal of Advanced Transportation*, vol. 2017, Article ID 6973089, 9 pages, 2017.
- [37] S. Joo and C. Oh, “A novel method to monitor bicycling environments,” *Transportation Research Part A: Policy and Practice*, vol. 54, pp. 1–13, 2013.
- [38] Z. Li, W. Wang, P. Liu, and D. R. Ragland, “Physical environments influencing bicyclists’ perception of comfort on separated and on-street bicycle facilities,” *Transportation Research Part D: Transport and Environment*, vol. 17, no. 3, pp. 256–261, 2012.
- [39] L. Bai, P. Liu, C.-Y. Chan, and Z. Li, “Estimating level of service of mid-block bicycle lanes considering mixed traffic flow,” *Transportation Research Part A: Policy and Practice*, vol. 101, pp. 203–217, 2017.
- [40] X. Chen, X. Fang, J. Ye, and T. Luttinen, “Classification criteria and application of level of service for bicycle lanes in China,” *Transportation Research Record*, vol. 2662, no. 1, pp. 116–124, 2017.
- [41] R. H. Blessing, “Outlier treatment in data merging,” *Journal of Applied Crystallography*, vol. 30, no. 4, pp. 421–426, 1997.

- [42] Z-Score, "Investopedia," 2023, <https://www.investopedia.com/terms/z/zscore.asp>.
- [43] W. Wang, C. Liu, and D. Zhao, "How much data are enough? A statistical approach with case study on longitudinal driving behavior," *IEEE Transactions on Intelligent Vehicles*, vol. 2, no. 2, pp. 85–98, 2017.
- [44] R. Koenker and G. Bassett, "Regression quantiles," *Econometrica*, vol. 46, no. 1, pp. 33–50, 1978.
- [45] X. Qin and P. E. Reyes, "Conditional quantile analysis for crash count data," *Journal of Transportation Engineering*, vol. 137, no. 9, pp. 601–607, 2011.
- [46] X. Qin, "Quantile effects of causal factors on crash distributions," *Transportation Research Record*, vol. 2279, no. 1, pp. 40–46, 2012.
- [47] X. Liu, M. R. Saat, X. Qin, and C. P. L. Barkan, "Analysis of U.S. freight-train derailment severity using zero-truncated negative binomial regression and quantile regression," *Accident Analysis & Prevention*, vol. 59, pp. 87–93, 2013.
- [48] S. Washington, M. M. Haque, J. Oh, and D. Lee, "Applying quantile regression for modeling equivalent property damage only crashes to identify accident blackspots," *Accident Analysis & Prevention*, vol. 66, pp. 136–146, 2014.
- [49] Q. Liu, J. Sun, Y. Tian, Y. Ni, and S. Yu, "Modeling and simulation of nonmotorized vehicles' dispersion at mixed flow intersections," *Journal of Advanced Transportation*, vol. 2019, Article ID 9127062, 19 pages, 2019.
- [50] S. K. Beura, H. Chellapilla, M. Panda, and P. K. Bhuyan, "Bicycle Comfort Level Rating (BCLR) model for urban street segments in mid-sized cities of India," *Journal of Transport & Health*, vol. 20, Article ID 100971, 2021.
- [51] S. Zhu and F. Zhu, "Cycling comfort evaluation with instrumented probe bicycle," *Transportation Research Part A: Policy and Practice*, vol. 129, pp. 217–231, 2019.
- [52] S. U. Jensen, "Pedestrian and bicyclist level of service on roadway segments," *Transportation Research Record*, vol. 2031, no. 1, pp. 43–51, 2007.
- [53] L. A. Elefteriadou, "The highway capacity manual 6th edition: a guide for multimodal mobility analysis," *ITEA Journal*, vol. 86, no. 4, 2016.
- [54] X. Liang, T. Zhang, M. Xie, and X. Jia, "Analyzing bicycle level of service using virtual reality and deep learning technologies," *Transportation Research Part A: Policy and Practice*, vol. 153, pp. 115–129, 2021.
- [55] A. R. Lawson, V. Pakrashi, B. Ghosh, and W. Y. Szeto, "Perception of safety of cyclists in dublin city," *Accident Analysis & Prevention*, vol. 50, pp. 499–511, 2013.
- [56] Y. Yuan, W. Daamen, B. Goñi-Ros, and S. P. Hoogendoorn, "Investigating cyclist interaction behavior through a controlled laboratory experiment," *Journal of Transport and Land Use*, vol. 11, no. 1, pp. 833–847, 2018.